Heat and Mass Transformation of Casson Hybrid Nano Fluid (MoS2 + ZnO) based on Engine Oil over a Stretched Wall with Chemical Reaction and Thermo-diffusion Effect

Shreedevi Madiwal and Neminath B. Naduvinamani *

Posted Date: 23 April 2024

doi: 10.20944/preprints202404.1522.v1

Keywords: Casson Hybrid nanofluid; Engine oil; Heat and Mass Transformation; Magnetic field; Soret effect; Chemical reaction

Article

Heat and Mass Transformation of Casson Hybrid Nano Fluid (MoS_2 + ZnO) based on Engine Oil over a Stretched Wall with Chemical Reaction and Thermo-Diffusion Effect

Shreedevi Madiwal and Neminath B. Naduvinamani *

Department of Mathematics, Gulbarga University, Kalaburagi 585106, INDIA
* Correspondence: naduvinamaninb@yahoo.co.in

Abstract: This study investigates the potential of a hybrid nanofluid composed of MoS_2 and ZnO nanoparticles dispersed in engine oil, aiming to enhance the properties of lubricant's chemical reaction with the Soret effect on stretching sheet under the influence of applied magnetic field. With the growing demand for efficient lubrication systems in various industrial applications, including automotive engines, the development of novel nanofluid-based lubricants presents a promising avenue for improving engine performance and longevity. However, the synergistic effects of hybrid nanoparticles in engine oil remain relatively unexplored. This research addresses this gap by examining the thermal conductivity, viscosity, and wear resistance of the hybrid nanofluid, shedding light on its potential as an advanced lubrication solution. By analyzing the dispersion stability and interaction mechanisms between nanoparticles and base oil, valuable insights are gained into the fundamental aspects governing the entertainment of hybrid nano lubricants. Overall, the objectives of studying hybrid nano lubricant MoS_2+ZnO with engine oil aim to advance the development of more efficient and durable lubrication solutions for automotive engines, contributing to improved reliability, fuel efficiency, and environmental sustainability. Governing non-linear partial differential equations are simplified as ordinary differential equations by utilizing similarity variables. MATLAB Bvp4c technique is used to solve the obtained linear ODE equations. The outputs are presented through graphs and tables for various state variables. The comparative survey in all the graphs is presented for the nanofluid (MoS_2/Engine oil) with the hybrid nanofluid (MoS_2+ZnO/Engine oil). These graphs show the effect of various parameters M, Q, β, Pr, Ec, Sc, Sr, Kp, Kr and ϕ_2 * (hybrid nano lubricant parameter). The velocity profile diminished against the values of M, Kp, and β. Temperature profile rising with Ec and Q. reciprocally goes down to Pr. The concentration profile incremented with the value of Sr and decremented with the value of Sc, and Kr. With the increasing value of ϕ_2 * both $f'(\eta)$ and $\theta(\eta)$ increases. But in $\theta(\eta)$ hybrid nanofluid slows down with the higher value of ϕ_2 *.

Keywords: casson hybrid nanofluid; engine oil; heat and mass transformation; magnetic field; soret effect; chemical reaction

1. Introduction

Researchers are continuously exploring novel combinations of nanoparticles and base fluids to enhance the thermal conductivity, convective heat transfer coefficient, and overall heat transfer performance of nanofluids. Recent studies have focused on optimizing the nanoparticle concentration, size, shape, and surface characteristics to achieve superior heat transfer enhancement. Hybrid nanofluids are being investigated for various thermal management applications, including cooling systems in electronics, heat exchangers, solar thermal collectors, and automotive cooling

 doi:10.20944/preprints202404.1522.v1

systems. The ability of hybrid nanofluids to improve heat transfer efficiency and thermal stability makes them promising candidates for addressing thermal management challenges in modern engineering systems. Computational modeling and numerical simulation techniques play a crucial role in predicting the heat and mass transfer characteristics of hybrid nanofluids.

Researchers are developing advanced computational models based on techniques such as computational fluid dynamics (CFD), molecular dynamics (MD), and lattice Boltzmann methods to simulate the behavior of hybrid nanofluids at the nanoscale and macroscopic levels. Despite the promising performance of hybrid nanofluids in laboratory settings, there are practical challenges related to scalability, stability over long-term usage, and cost-effectiveness that need to be addressed for their widespread industrial applications. Researchers are working on developing scalable synthesis methods, improving nanoparticle dispersion techniques, and conducting cost-benefit analyses to facilitate the transition of hybrid nanofluids from the lab to real-world applications. Umair Khan et al. [1] studies aimed at offering a computational solution for the flow of a wall jet (WJ) incorporating thermal and mass transportation phenomena. Their study focuses on a colloidal suspension consisting of SAE50 and zinc oxide nanoparticles, which are submerged in a Brinkman-extended Darcy model. Belal et al. [2] examined how the utilization of blended individual and hybrid nano additives, including graphene nanoplatelets, ZnO, and an ionic liquid (IL) named Trihexyltetradecylphosphonium bis(2,4,4-trimethylpentyl) phosphinate, affects the rheological, tribological, and physical properties of rapeseed oil.

The work of Zia Ullah et. al. [3] primarily focuses on the enhanced rate of chemical processes in the magneto-nanofluid flow and the physical manifestation of viscous dissipation. Oriana Palma Calabokis et al. [4] studied the problem to enhance the wear and friction properties of frictional components—which are mostly found in rolling bearings, gearboxes, and engines—metal conditioners (MC) are added to lubricants. Its primary objective in entering the Brazilian market is to increase its market share in internal combustion engines. Their investigation focused on the effects of mixing metal conditioners (MC) with SAE 5W-30 API SN commercial engine oil on the thermal and rheological characteristics. Zawar Hussain et al. [5] investigated the flow of copper and alumina nanoparticles mixed with sodium alginate-based Casson hybrid nanofluid across a stretching sheet. In this problem, they assumed convective and slip boundary conditions. Najiyah Safwa Khashi'ie et al. [6] investigated the presence of velocity slip and convective conditions; a hybrid Cu-Al_2O_3/water nanofluid flows towards a stretching/shrinking sheet. It is considered necessary to maintain an adequate wall mass suction to maintain the shrinking flow through a permeable sheet. Bilal et al. [7] described features of a three-dimensional boundary layer flow of Williamson fluid that is restricted by a bidirectional stretched surface in magnetohydrodynamics (MHD). It is assumed that the fluid conductivity varies with temperature. Heat transfer via generative/absorptive processes is also taken into account. Muhammad Ramzan et al. [8] simulated the three-dimensional MHD flow over an extending sheet of micropolar and Williamson fluids. Their study examines activation energy and heat radiation influence. Also, Brownian motion, chemical reaction, and thermal migration impact are calculated. Numerical investigation is conducted on continuous three-dimensional mixed convection flow of nanofluids under slip circumstances over a permeable vertical stretching/shrinking sheet in magnetohydrodynamics (MHD) by Anuar Jamaludin et al. [9]. In their study, two types of nanofluids, namely Cu-water and Ag-water, were examined. Ishtiaq Khan et al. [10] studied the utilization of nanoliquids holds significant potential across various fields including heat exchangers, food processing, biomedicine, cooling electronics, and transportation. Their analysis takes into account of the impact of velocity slips, zero mass flux, and thermal convection. Interestingly, the zero-mass flux situation at the wall negates the hybrid nano liquid flow's wall mass transfer rate.

Nanofluids hold considerable importance for researchers owing to their notably high heat transfer rates, making them valuable for industrial applications Tanzila Hayat et al. [11]. Recently, a novel class of nanofluids, termed "hybrid nanofluids," has emerged, aiming to further augment heat transfer rates. The newly developed 3D model is utilized to investigate the influence of heat generation, heat radiation, and chemical reaction on a stretching wall with rotation. Awatif

 doi:10.20944/preprints202404.1522.v1

Alhowaity et al. [12] examined the energy and mass transfer rates in the flow of a Williamson hybrid nanofluid (NF) is a porous surface that is stretched and contains silver (Ag) and magnesium oxide (MgO) nanoparticles (NPs). By dispersing magnesium oxide (MgO) and silver (Ag) nanoparticles in the base fluid (engine oil), the hybrid nanofluid is created. Additionally, the present analysis investigates the effects of a constant magnetic field heat source and heat dissipation. The introduction of the hybrid nanofluid concept has sparked advancements in enhancing heat transfer within boundary layer flows Suriya Uma Devi et al. [13]. In their study the novel thermo physical properties models have been developed and experimental thermal conductivity values are compared with our proposed model. Two distinct types of fluids, specifically Hybrid nanofluid (Cu-Al_2O_3/Water) and Nanofluid (Cu/Water), are utilized in the investigation of move past a stretching sheet.

Ram Prakash Sharma et al. [14] study compares the effects of both linear and nonlinear stretching sheets on the heat transfer properties over a curved surface spiralling in a circle at different radial distances. The impacts of the Soret-Dufour phenomenon in the presence of injection velocity and heat source/sink are also examined in this article. Silver and copper oxide hybrid nanoparticles are used, with water serving as the base fluid. The investigation is conducted on the flow of a methanol-based hybrid fluid over a curved stretching sheet by Revathi et al. [15] study by considering the cross-diffusion effects (Soret–Dufour numbers) and also activation energy. Further, the visualization of entropy generation in the fluid flow is also performed. For instance, specific heat and thermal conductivity exhibit an increase at higher temperatures. Experimental research has revealed that methanol-based hybrid nanofluids ($CH_3OH + SiO_2 + Al_2O_3$) effectively increase the rate of absorption of CO_2 in a tray column absorber. Motahar Reza et al. [16] conducted a numerical study to examine the effects of Soret and Dufour phenomena on the creation of entropy in a (AlN-Al2O3) hybrid nanofluid flowing across a stretched plate through a permeable medium saturated with hybrid nanofluid. To explore the impact of thermo-diffusion and diffuse-thermal effects on entropy generation in this scenario, a transverse magnetic field has been employed. Their study investigates the enhancement of heat transfer rates using a mixture of Aluminium Nitride (AlN) and Alumina (Al_2O_3) nanoparticles. The demand for improved thermal conductivity to handle boosting the density of heat in miniature and various technical procedures has prompted an examination of the thermal transport properties of hybrid nanofluids by Asmat Ullah Yahya et al. [17] . In this context, MoS_2 and ZnO are combined as a highly diluted homogeneous composition within a great quantity of engine oil. This colloidal fluid flows over a stretched sheet through a porous media, in the presence of heat transformation. The study of Shami Alsallami et al. [18] goals at enhancement of engine oil's thermal characteristics by adding a suspension of Williamson hybrid nanofluid. Zinc oxide (ZnO) and molybdenum disulfide (MoS_2) are suspended in the hybrid nanofluid. Viscosity dissipation properties and external heat sources are added to increase the system's heating capability. The problem studied by Sreedevi et al. [19] entails the analysis of thermal and mass transformation in an inconstant magneto-hydrodynamic movement of a hybrid nanofluid on a stretching sheet. The scenario includes the presence of chemical reactions, suction, slip effects, and thermal radiation.

The work of Mubashar Arshad et al. [20] examines the three-dimensional magneto-hydrodynamic nanofluid flow over two stretching surfaces, taking into account the effects of thermal radiation and chemical reactions in addition to the effect of an inclining magnetic field. In their comparative study, several rotational nanofluids and hybrid nanofluids with a constant angular velocity are investigated. The analysis of a nonlocal fractional model for viscous nanofluid with hybrid nanostructure is presented by Yu-Ming Chu et al. [21]. To develop a hybrid nanofluid, copper (Cu) and aluminium oxide (Al_2O_3) nanoparticles were mixed and distributed within a base fluid of water (H_2O). Within a microchannel, the magnetohydrodynamic (MHD) free convection flow of the Cu-Al_2O_3-H_2O nanofluid was examined. The flow of an incompressible hybrid nanofluid over a rotating disk that is endlessly impermeable is examined by Tassaddiq et al. [22]. To improve the examination of the nanoliquids flow's fine point, the effect of a magnetic field has been included. In their work, magnetic ferrite nanoparticles and carbon nanotubes (CNTs) contained in a carrier fluid like water are studied in relation to the classical von Karman flow over a spinning disk. The standard fluid water which suspends two different kinds of hybrid nanoparticles—single-walled CNTs

 doi:10.20944/preprints202404.1522.v1

(SWCNTs) and multi-walled CNTs (MWCNTs) considered in the study by Shanmugapriya et al. [23]. To further explore the complexities of hybrid nanofluid flow, the effects of heat radiation, activation energy, and magnetic fields have been included in addition to binary chemical reactions.

The study of Sohail Ahmad et al. [24] revels that, the hybrid nanofluids demonstrate superior mechanical resistance, physical strength, chemical stability, thermal conductivity, and other properties in comparison to individual nanoliquids. In their study, it is aimed to introduce a novel investigation into the magnetohydrodynamic (MHD) flow of hybrid nanoparticles through a permeable medium, considering viscous dissipation, as they pass over a stretching surface. The study of Abdulmajeed Almaneea [25] examines the impact of hybrid nanoparticles on thermal and mass transformation in both heterogeneous and homogeneous chemical reactions. The Williamson parameter can have a notable impact on momentum transport. The Darcy-Forchheimer flow of a Casson hybrid nanofluid through a continuously expanding curved surface was studied by Gohar et al. [26]. The Darcy-Forchheimer effect characterizes the viscous fluid flow within a porous medium. Hybrid nanofluids are created using carbon nanotubes (CNTs) in cylindrical form and iron oxide. An inquiry is underway to elucidate the flow behavior of a Ree-Eyring hybrid nanofluid under stretching flow conditions by Ali et al. [27]. Studied SiO_2 and GO are under investigation for their potential use as hybrid nanoparticles in combination with carboxymethyl cellulose (CMC) in water at low concentrations. A concentration range between 0.0 and 0.4 % is recommended for use as the base fluid (CMC-water). The work of Wei-Feng Xia et al. [28] focuses on the three-dimensional nonlinear mixed convective boundary layer flow of a micropolar hybrid nanofluid under numerous slip conditions and in the presence of microorganisms along the narrowing surface. The goal of their study is to learn more about carbon nanotubes (CNTs), which are very popular because of their consistent physicochemical properties, high thermal and electrical conductivities, mechanical and chemical stability, and lightweight design. The objective of the research of Saeed Dinarv et al. [29] analyze the Falkner-Skan problem, which is the steady laminar incompressible two-dimensional boundary layer flow of a TiO_2-CuO/water hybrid nanofluid over a fixed or moving wedge or corner. One-phase hybrid nanofluids are modelled using a novel mass-centric approach in which the masses of the base fluid, the first and second nanoparticles, and both are regarded as essential inputs for establishing the effective thermophysical parameters of the hybrid nanofluid. The extension of a hybrid nanofluid made of Cu, Al_2O_3, and H_2O between two infinite vertical parallel plates is covered in the study of Muhammad Saqib et al. [30]. studied the energy equation in conjunction with the Brinkman-type fluid model to depict the flow phenomena between two parallel plates filled with hybrid nanofluids.

Overall, research in the field of heat and mass transfer of hybrid nanofluids continues to evolve, driven by the demand for efficient thermal management solutions in various industrial sectors. As advancements in nanomaterial synthesis, characterization techniques, and computational modeling tools progress, hybrid nanofluids are expected to play an increasingly important role in enhancing heat transfer efficiency and sustainability in diverse engineering applications. The present study aims at understanding the heat and mass transformation of Casson hybrid nano fluid ($MoS_2 + ZnO$) based with engine oil over a stretched wall with chemical reaction and thermo-diffusion effects.

2. Materials and Methods

Consider a mathematical formulation for two two-dimensional (2D) in-compressible Casson hybrid nanofluids past a stretched surface. Cartesian coordinates (x, y) and velocity components (u, v) with a fluid flow arrangement are shown in Figure 1 as the problem's design. The interface of the applied magnetic field with dynamic viscosity and a porous media is used to study mass diffusion and heat transfer. The magnetic field B_0 is applied along the x-axis. The governing equations of this problem are as follows:

 doi:10.20944/preprints202404.1522.v1

$$\frac{\partial u}{\partial x}+\frac{\partial v}{\partial y}=0 \tag{1}$$

$$u\frac{\partial u}{\partial x}+v\frac{\partial u}{\partial y}=\frac{\mu_{hnf}}{\rho_{hnf}}\left(1+\frac{1}{\beta}\right)\frac{\partial^2 u}{\partial y^2}-\frac{\sigma B_0^2 u}{\rho_{hnf}}-\frac{\mu_{hnf}}{\rho_{hnf}}\frac{u}{k^*} \tag{2}$$

$$u\frac{\partial T}{\partial x}+v\frac{\partial T}{\partial y}=\frac{k_{hnf}}{\left(\rho C_p\right)_{hnf}}\frac{\partial^2 T}{\partial y^2}+\frac{\mu_{hnf}}{\left(\rho C_p\right)_{hnf}}\left(\frac{\partial u}{\partial y}\right)^2+\frac{Q_0}{\left(\rho C_p\right)_{hnf}}\left(T-T_\infty\right) \tag{3}$$

$$u\frac{\partial C}{\partial x}+v\frac{\partial C}{\partial y}=D_m\frac{\partial^2 C}{\partial y^2}+\frac{D_m K_T}{T_m}\frac{\partial^2 T}{\partial y^2}-K(C-C_\infty) \tag{4}$$

Boundary conditions:

$$\left.\begin{array}{l} u=U_w=ax, \quad v=0, \quad T=T_w, \quad C=C_w, \quad as \quad y=0 \\ u\to 0, \quad T\to T_\infty, \quad C\to C_\infty, \quad as \quad y\to\infty \end{array}\right\} \tag{5}$$

The flow of the hybrid nanofluids are explained here with the help of thermo-physical characteristics. ϕ^*, ϕ_1^* and ϕ_2^* are the volume fraction of hybrid nano fluids. To create the required nanolubricant, ZnO nanoparticles are mixed with 0.01 vol of MoS2/engine oil. Considering $\phi_1^*=0.04$ and $\phi_2^*=0$ for MoS_2 /Engine oil in this model. For hybrid nano lubricant $\phi_1^*=0.03$ and $\phi_2^*=0.01$ to yield MoS_2+ZnO /Engine oil over all the research.

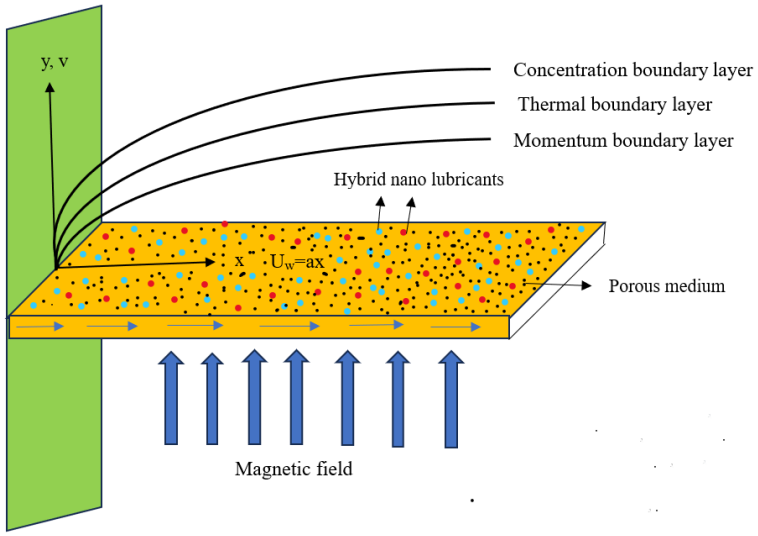

Figure 1. Schematic diagram of the problem.

The flow of the hybrid nanofluids are explained here with the help of thermo-physical characteristics. ϕ^*, ϕ_1^* and ϕ_2^* are the volume fraction of hybrid nano fluids. To create the required nanolubricant, ZnO nanoparticles are mixed with 0.01 vol of MoS2/engine oil. Considering $\phi_1^*=0.04$ and $\phi_2^*=0$ for MoS_2 /Engine oil in this model. For hybrid nano lubricant $\phi_1^*=0.03$ and $\phi_2^*=0.01$ to yield MoS_2+ZnO /Engine oil over all the research. To be explicit, Table 1 presents the

 doi:10.20944/preprints202404.1522.v1

valuable thermo-physical characteristics of both nano lubricants and hybrid nano lubricants. The fundamental thermo-physical properties of nanofluids are derived from the literature review mentioned below. Table 2 provides information on the thermophysical properties of engine oil used as the base fluid.

Table 1. Engine oil base fluid and nanoparticle thermo-physical properties [13].

Physical properties	MoS_2	ZnO	Engine oil
$\rho(kg.m^{-3})$	5060	5600	884
$C_p/j(kg.k)$	397.21	495.2	1910
$W.k/m.k$	904.4	13	0.144

Table 2. Nano lubricant and hybrid nano lubricants thermo-physical properties [13].

Properties	Nanofluid	Hybrid Nnofluid
μ (viscosity)	$\mu_{nf} = \dfrac{\mu_{nf}}{(1-\phi^*)^{2.5}}$	$\mu_{hnf} = \left[\dfrac{\mu_f}{(1-\phi_1^*)^{2.5}(1-\phi_1^*)^{2.5}}\right]$
ρ(density)	$\rho_{nf} = \rho_f(1-\phi^*) + \phi^* \dfrac{\rho_s}{\rho_f}$	$\rho_{hnf} = \left[\begin{array}{l}\rho_f(1-\phi_2^*)\left((1-\phi_1^*) + \phi_1^* \dfrac{\rho_{s1}}{\rho_f}\right) \\ +\phi_2^* \rho_{s2}\end{array}\right]$
ρC_p(Heat capacity)	$(\rho C_p)_{nf} = (\rho C_p)_f \left(\begin{array}{l}(1-\phi^*) \\ +\phi^* \dfrac{(\rho C_p)_s}{(\rho C_p)_f}\end{array}\right)$	$(\rho C_p)_{hnf} = \left[\begin{array}{l}(\rho C_p)_f(1-\phi_2^*)\left(\begin{array}{l}(1-\phi_1^*) \\ +\phi_1^* \dfrac{(\rho C_p)_{s1}}{(\rho C_p)_f}\end{array}\right) \\ +\phi_2^*(\rho C_p)_{s2}\end{array}\right]$
k(Thermal conductivity)	$\dfrac{k_{nf}}{k_f} = \dfrac{k_s + (s_f - 1)k_f - (s_f - 1)\phi^*(k_f - k_s)}{k_s + (s_f - 1)k_f + \phi^*(k_f - k_s)}$	$\dfrac{k_{hnf}}{k_{bf}} = \left[\dfrac{k_{s2} + (s_f - 1)k_{bf} - (s_f - 1)\phi_2^*(k_{bf} - k_{s2})}{k_{s2} + (s_f - 1)k_{bf} + \phi^*(k_{bf} - k_{s2})}\right]$ *where* $\dfrac{k_{bf}}{k_f} = \left[\dfrac{k_{s1} + (s_f - 1)k_f - (s_f - 1)\phi_1^*(k_f - k_{s1})}{k_{s1} + (s_f - 1)k_f + \phi^*(k_f - k_{s1})}\right]$

2.1. Similarity Variables

In order to solve equations (1)–(4) subject to the boundary conditions (5), the similarity transformation and stream function are mentioned. They're provided by

$$\left.\begin{array}{l} u = axf'(\eta), \quad v = \left(\sqrt{-a\upsilon_f}\right) f(\eta), \quad \eta = \sqrt{\dfrac{a}{\upsilon_f}}\, y, \\ \theta(\eta) = \dfrac{T - T_\infty}{T_w - T_\infty}, \quad \phi(\eta) = \dfrac{C - C_\infty}{C_w - C_\infty} \end{array}\right\} \tag{6}$$

The transformed ordinary differential equations are:

$$\left(1 + \frac{1}{\beta}\right) f'''(\eta) - Kpf'(\eta) - S_4 Mf'(\eta) - S_1\left[f'^2(\eta) - f(\eta) f''(\eta)\right] = 0 \tag{7}$$

$$\theta''(\eta) + \frac{\Pr}{S_6}\left(\frac{Ec}{S_5} f''^2(\eta) + Q\theta(\eta) + f(\eta)\theta'(\eta)\right) = 0 \tag{8}$$

 doi:10.20944/preprints202404.1522.v1

$$\phi''(\eta) - ScKr\phi(\eta) - Scf(\eta)\phi'(\eta) - ScSr\theta'' = 0 \tag{9}$$

$$\left.\begin{aligned} f(\eta) = 0, \quad f'(\eta) = 1, \quad \theta(\eta) = 1, \quad \phi(\eta) = 1, \quad at \quad \eta = 0 \\ f'(\eta) \to 0, \quad \theta(\eta) \to 0, \quad \phi(\eta) \to 0, \quad as \quad \eta \to \infty. \end{aligned}\right\} \tag{10}$$

where M denotes the magnetic parameter, Sc Schmidt number, Kp denotes the porosity parameter, Sr is the Soret effect parameter, Kr is the chemical reaction parameter, Pr represents Prandtl number, Eckert number is Ec, Q denotes heat source, where β is the Casson fluid parameter.

$$M = \frac{\sigma B_0^2}{\rho_f a}, \quad Kp = \frac{\upsilon_f}{ak^*}, \quad Ec = \frac{a^2 x^2}{(C_p)_f (T_w - T_\infty)}, \quad \Pr = \frac{\upsilon_f (\rho C_p)_f}{k_f},$$

$$Q = \frac{Q_0}{(C_p)_f (T_w - T_\infty)}, \quad Sc = \frac{\upsilon_f}{D_m}, \quad Sr = \frac{D_m K_T}{T_m \upsilon_f}\left(\frac{T_w - T_\infty}{C_w - C_\infty}\right), \quad Kr = \frac{K}{a}$$

Also,

$$S_1 = (1-\phi_1^*)^{2.5}(1-\phi_2^*)^{2.5}\left[(1-\phi_2^*)\left((1-\phi_1^*) + \phi_1^* \frac{\rho_{s1}}{\rho_f}\right) + \phi_2^* \frac{\rho_{s2}}{\rho_f}\right]$$

$$S_2 = \left[(1-\phi_2^*)\left((1-\phi_1^*) + \phi_1^* \frac{\rho_{s1}}{\rho_f}\right) + \phi_2^* \frac{\rho_{s2}}{\rho_f}\right]$$

$$S_3 = (1-\phi_2^*)\left((1-\phi_1^*) + \phi_1^* \frac{(\rho C_p)_{s1}}{(\rho C_p)_f}\right) + \phi_2^* \frac{(\rho C_p)_{s2}}{(\rho C_p)_f}$$

$$S_4 = (1-\phi_1^*)^{2.5}(1-\phi_2^*)^{2.5}$$

$$S_5 = \left[(1-\phi_2^*)\left((1-\phi_1^*) + \phi_1^* \frac{(\rho C_p)_{s1}}{(\rho C_p)_f}\right) + \phi_2^* \frac{(\rho C_p)_{s2}}{(\rho C_p)_f}\right]\left((1-\phi_1^*)^{2.5}(1-\phi_2^*)^{2.5}\right)$$

$$S_6 = \frac{k_{hnf}}{k_{bf}} = \left[\frac{k_{s2} + (s_f - 1)k_{bf} - (s_f - 1)\phi_2^*(k_{bf} - k_{s2})}{k_{s2} + (s_f - 1)k_{bf} + \phi^*(k_{bf} - k_{s2})}\right]$$

The Physical quatities of intrest are given below

$$\left.\begin{aligned} Cf_x = \frac{\tau_w}{\rho_f U_w^2}, \quad Nu_x = \frac{xq_w}{k_f (T_w - T_\infty)}, \quad Sh_x = \frac{xq_m}{D_B (C_w - C_\infty)}, \\ \tau_w = \mu_{hnf}\left(\frac{\partial u}{\partial y}\right), \quad q_w = k_{hnf}\frac{\partial T}{\partial y}, \quad q_m = -D_B \frac{\partial C}{\partial y}, \quad at \quad y = 0 \end{aligned}\right\} \tag{11}$$

Utilizing similarity transformation, we get

Preprints.org (www.preprints.org) | NOT PEER-REVIEWED | Posted: 23 April 2024 doi:10.20944/preprints202404.1522.v1

$$\left.\begin{aligned} Cf_x\left(2\,\mathrm{Re}_x\right)^{1/2} &= \frac{\mu_{hnf}}{\mu_f} f''(0) \\ Nu_x\,\mathrm{Re}_x^{-1/2} &= \frac{k_{hnf}\theta'(0)}{k_f} \\ Sh_x\,\mathrm{Re}_x^{-1/2} &= -\phi'(0) \end{aligned}\right\} \tag{12}$$

where Re_x is a local Reynolds number, Cf_x is skin friction co-effeciant, Nu_x is local Nussult number, and Sh_x is Sherwood number.

3. Numerical Procedure

This intended hybrid nanofluid flow has a naturally non-linear boundary value problem, which is represented by equations (1) through (4). Finding a closed form solution is really difficult, as usual. In order to arrive at an approximate numerical solution for the problem, a numerical method that uses the MATLAB Bvp4c technique is employed. The higher order derivatives in this scheme must be reduced to first order in the following manner:

$$\left.\begin{aligned} f(\eta) &= \varepsilon_1 \\ f'(\eta) &= \varepsilon_2 \\ f''(\eta) &= \varepsilon_3 \\ f'''(\eta) &= \varepsilon_3' \end{aligned}\right\} \tag{13}$$

$$\varepsilon_3' = \left(\frac{1}{1+1/\beta}\right)\left[Kp\varepsilon_2 + S_4 M\varepsilon_2 + S_1\left(\varepsilon_2^2 - \varepsilon_1\varepsilon_3\right)\right] \tag{14}$$

$$\left.\begin{aligned} \theta(\eta) &= \varepsilon_4 \\ \theta'(\eta) &= \varepsilon_5 \\ \theta''(\eta) &= \varepsilon_5' \end{aligned}\right\} \tag{15}$$

$$\varepsilon_5' = \frac{-\mathrm{Pr}}{S_6}\left[\frac{Ec}{S_5}\varepsilon_3^2 + Q\varepsilon_4 + \varepsilon_1\varepsilon_5\right] \tag{16}$$

$$\left.\begin{aligned} \phi(\eta) &= \varepsilon_6 \\ \phi'(\eta) &= \varepsilon_7 \\ \phi''(\eta) &= \varepsilon_7' \end{aligned}\right\} \tag{17}$$

$$\varepsilon_7' = ScKr\varepsilon_6 - Sc\varepsilon_1\varepsilon_2 + \frac{ScSr\,\mathrm{Pr}}{S_6}\left[\frac{Ec}{S_5}\varepsilon_3^2 + Q\varepsilon_4 + \varepsilon_1\varepsilon_5\right] \tag{18}$$

 doi:10.20944/preprints202404.1522.v1

4. Result and Disscusion

In two cases, numerical solutions are computed, namely:

(i) MoS_2 /Engine oil (simple nano lubricant) and

(ii) ZnO + MoS_2 /Engine oil (hybrid nano lubricant).

According to Table 3, the above results can be verified if they compare reasonably with previous *Pr* results in limiting cases. In Figures 2–12, two results are presented for single nano lubricant (MoS_2/Engine oils) and for hybrid nano lubricant (MoS_2/Engine oils + ZnO). Figures 2 and 3 depicts the effects of magnetic characteristics parameters *M* and porosity parameters *Kp* on nondimensional horizontal velocity component f′ (η) respectively. Increasing these two parameters (*M* and *Kp*) dramatically slows down the flow of both nano lubricant (single nano lubricants as well as hybrid nano lubricants). According to physical principles, a larger value of *M* indicates a greater Lorentz force opposing the flow. The parameter *Kp* also corresponds to the lower porosity of the medium and higher resistance to flow with higher inputs.

Figure 4 represents the effect of the Casson lubricant parameter on the velocity. Rising Casson fluid parameter value decreases the velocity profile due to its shear-thinning property, hence, the wall thickness decreases. Figure 5 shows the results of the Prandtl number on the thermal profile. The value of *Pr* increases temperature profile decreases. Hence Increasing Pr results in a decrease in the thermal diffusivity of the fluid, which further reduces the thickness of the thermal boundary layer. Furthermore, compared to the single nanofluid, the hybrid nanofluid's velocity has been observed to be slower. Figure 6 represents the effect of heat source parameter *Q* on the temperature profile. Increases the temperature profile with increasing value of heat source parameter *Q*. Figure 7 represents the effect of Eckert number on the temperature profile. The temperature profile increases with the increasing value of *Ec.* The conversion of mechanical energy to heat energy through thermal dissipation is represented by the greater Eckert number. Furthermore, it was noted that nanofluids have a higher temperature than other nanofluids. This is because hybrid nanofluids have higher thermal conductivities. Figure 8 represents the effects of Schmidt number on the concentration profile. Increasing the value of the Schmidt number the concentration profile decreases.

Figure 9 shows the Soret effect on the concentration profile. Incremented Soret number increases the concentration profile, because the concentration is affected by the temperature gradient. Physically higher value of the Soret number corresponds to a higher temperature gradient which results in higher convection flow and hence the concentration profile increases. Figure 10 shows the chemical reaction (*Kr)* on the concentration profile. Increasing the values of *Kr*, decreases the concentration profile due to consumption character of this chemical reaction, hence concentration profile decreases.

Figures 11 and 12. It is discovered that as augmentation occurs, the velocity *f′ (η)* decreases. ϕ_2 * and the temperature rises till ϕ_2 *=0.4 but the temperature is slower with ϕ_2 *>0.4 due to mass flux and thermal diffusion. The flow is being slowed down because of the viscosity, which is increases ϕ_2 and has the effect of slowing down the flow. Moreover, Table 4 shows the skin fraction profile *- f′′ (0)* results for the various inputs *M, Kp,* and *β* in ZnO + MoS_2/Engine oil (hybrid nanofluid) variation. It is seen that *M, Kp,* and *β* rise directly for the absolute values of *- f′′ (0)* because the fluid flow slows down due to the conflicting forces of the electromagnetic interaction and the medium's porosity. The absolute value of the Nusselt number -*θ*′ (0) increases with progressing values of *Pr*, Table 5 provides information about the Prandtl number *Pr*. Also, it is noted that *-θ′(0)* decreases reciprocally with Eckert number *Ec* and heat source parameter *Q*. The value of Sherwood number $-\phi'(0)$ increases with *Ec, Kr*, and *Q* are shown in Table 6. It is also observed that $-\phi'(0)$ decreases to *Pr, Sc*, and *Sr.*

 doi:10.20944/preprints202404.1522.v1

Table 3. Comparison of (-θ (0)) with the results of Asmat Ullah et al. [13], Shami A.M. et al. [14], and P. shreedevi et al. [15], for various values of (Pr), $\phi_1^* = 0$ and $\phi_2^* = 0$ all r maining parameters zero.

Pr	Asmat Ullah et al. [13]	Shami A.M. et al. [14]	P. shreedevi et al. [15]	Our results
2.0	0.9112	0.91138	0.911341	0.911325
6.13	1.7597	1.75965	1.759676	1.759671
7.0	1.8953	1.8955	1.895397	1.895393
20.0	3.3540	-	3.353915	3.353921

Table 4. Results for Skin friction factor - $f''(\eta)$.

M	Kp	β	$-f''(\eta)$
0.0	0.5	0.5	0.7256
0.5			0.8227
1.0			0.9097
1.5	0.1		0.9191
	0.3		0.9547
	0.5		0.9889
	0.5	0.1	0.5170
		0.2	0.6993
		0.3	0.8228

Table 5. Results for Nusselt number - $\theta'(\eta)$.

Pr	Q	Ec	$-\theta'(\eta)$
7.0	0.01	0.1	1.5082
8.0			1.6176
10.0			1.8150
7.0	0.02		1.4899
	0.05		1.4341
	0.09		1.3574
	0.01	0.15	1.3899
		0.2	1.2715
		0.25	1.1532

Table 6. Results for Sherwood number $-\phi'(\eta)$.

Pr	Ec	Sc	Sr	Kr	Q	$-\phi'(\eta)$
6.3	0.1	0.4	0.8	0.2	0.01	0.0643
7.0						0.0396
7.5						0.0227
7.0	0.2					0.1128
	0.25					0.1494
	0.3					0.1860
	0.1	2.5				0.0735
		3.0				0.0624
		3.5				0.0511
		0.4	0.5			0.1848
			0.6			0.1364
			0.7			0.0880
			0.8	0.3		0.1002

 doi:10.20944/preprints202404.1522.v1

	0.4		0.1541
	0.5		0.2031
	0.2	0.02	0.0453
		0.04	0.0568
		0.06	0.0685

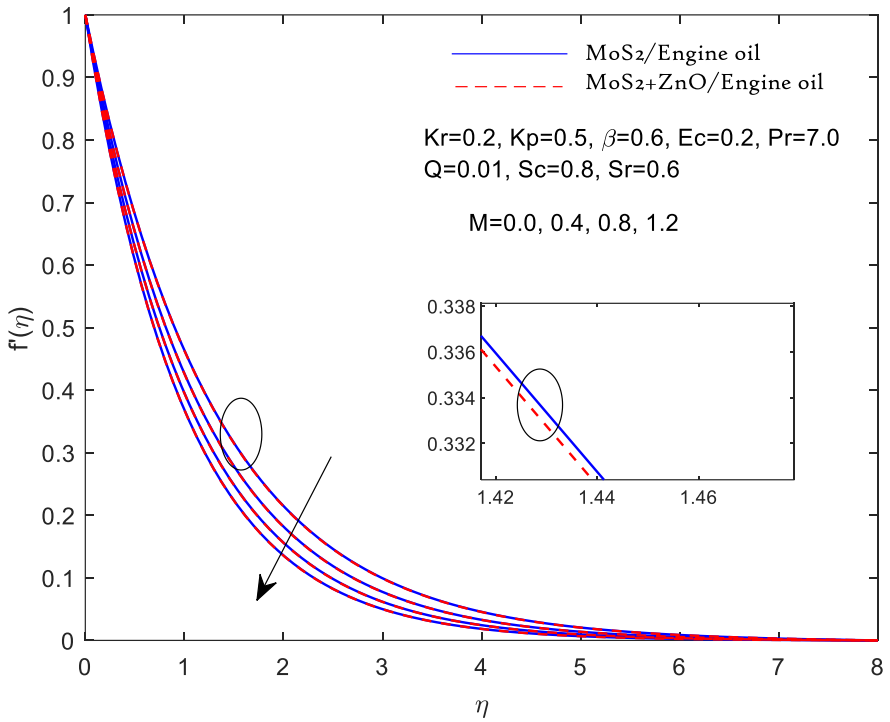

Figure 2. Velocity $f'(\eta)$ fluctuation with M.

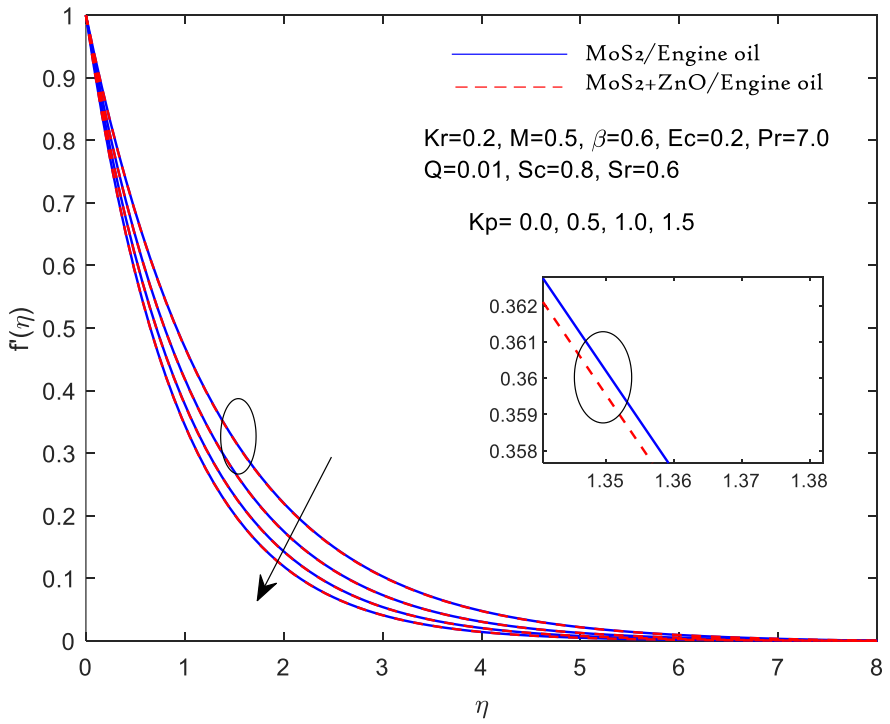

Figure 3. Velocity $f'(\eta)$ fluctuation with Kp.

Preprints.org (www.preprints.org) | NOT PEER-REVIEWED | Posted: 23 April 2024 doi:10.20944/preprints202404.1522.v1

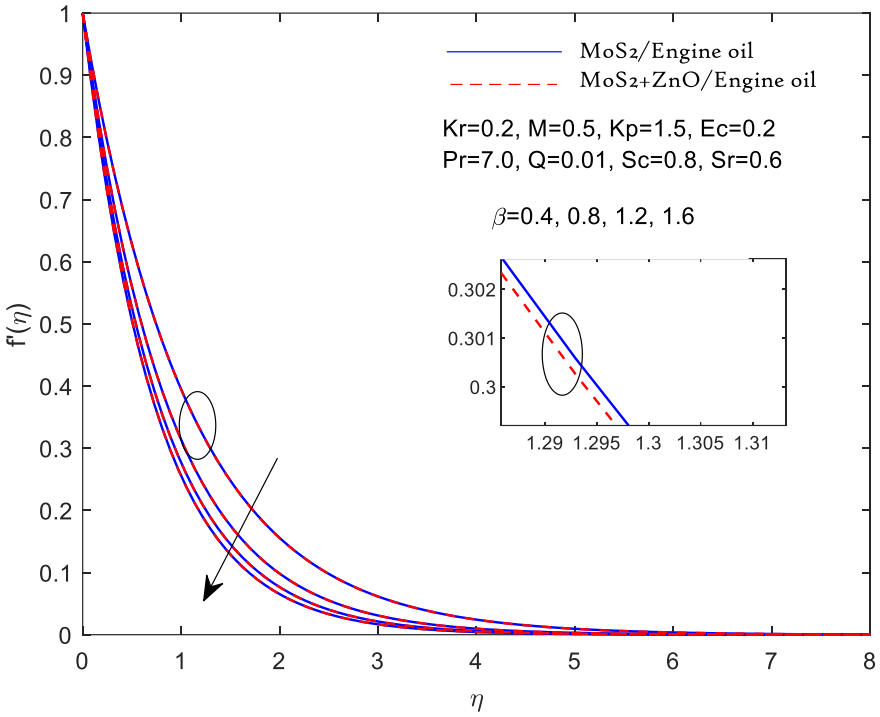

Figure 4. Velocity $f'(\eta)$ fluctuation with β.

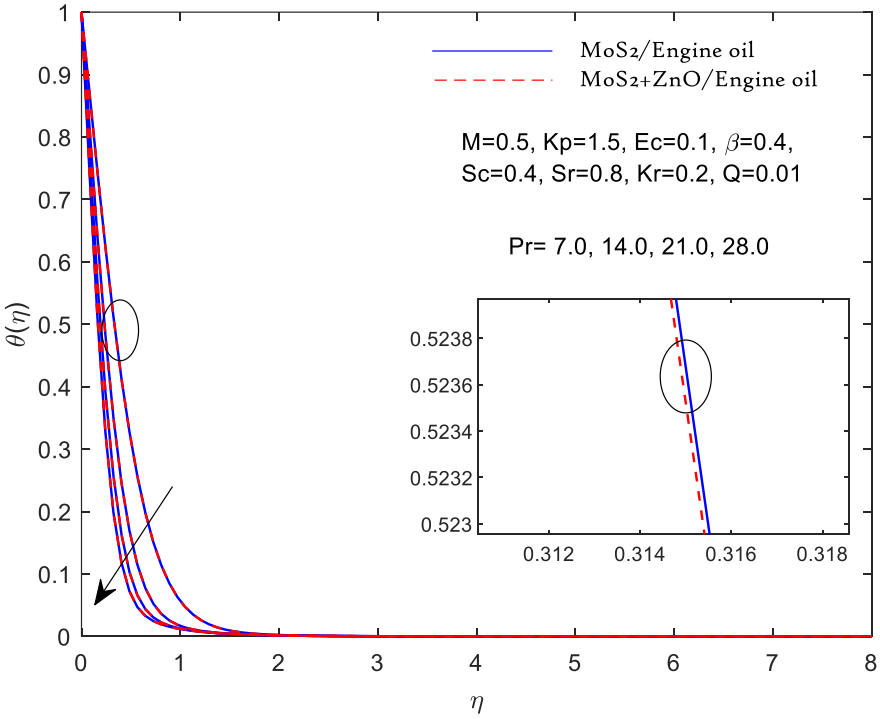

Figure 5. $\theta(\eta)$ fluctuation with Pr.

Preprints.org (www.preprints.org) | NOT PEER-REVIEWED | Posted: 23 April 2024 doi:10.20944/preprints202404.1522.v1

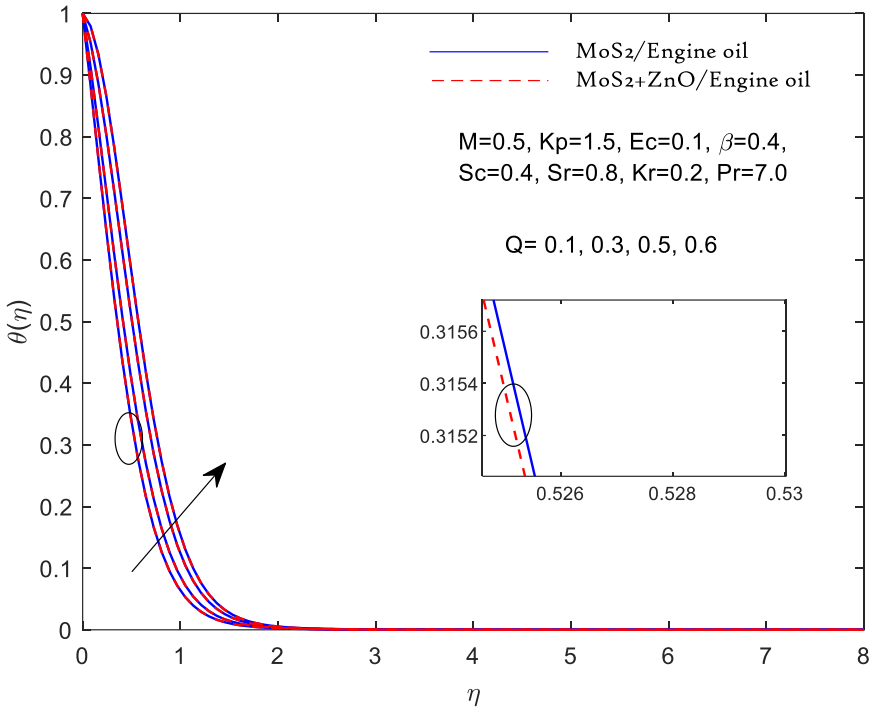

Figure 6. $\theta(\eta)$ fluctuation with Q.

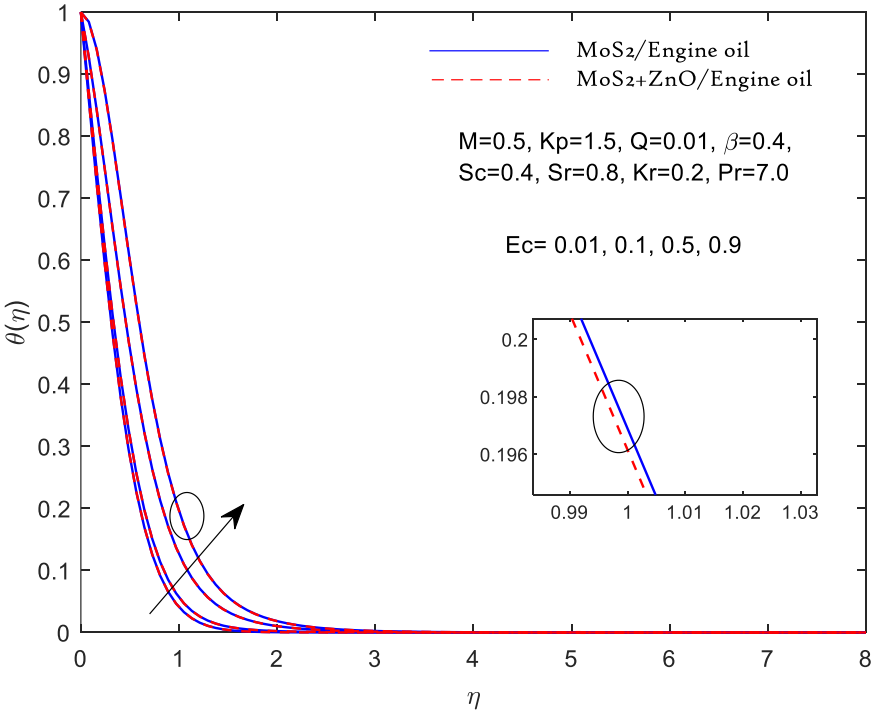

Figure 7. $\theta(\eta)$ fluctuation with Ec.

Preprints.org (www.preprints.org) | NOT PEER-REVIEWED | Posted: 23 April 2024 doi:10.20944/preprints202404.1522.v1

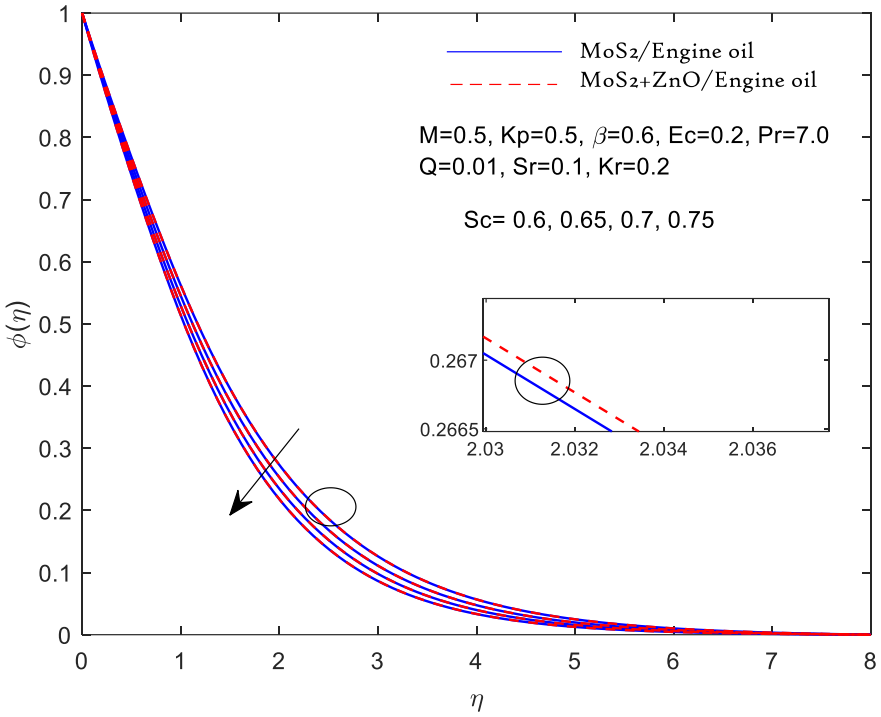

Figure 8. fluctuation with *Sc*.

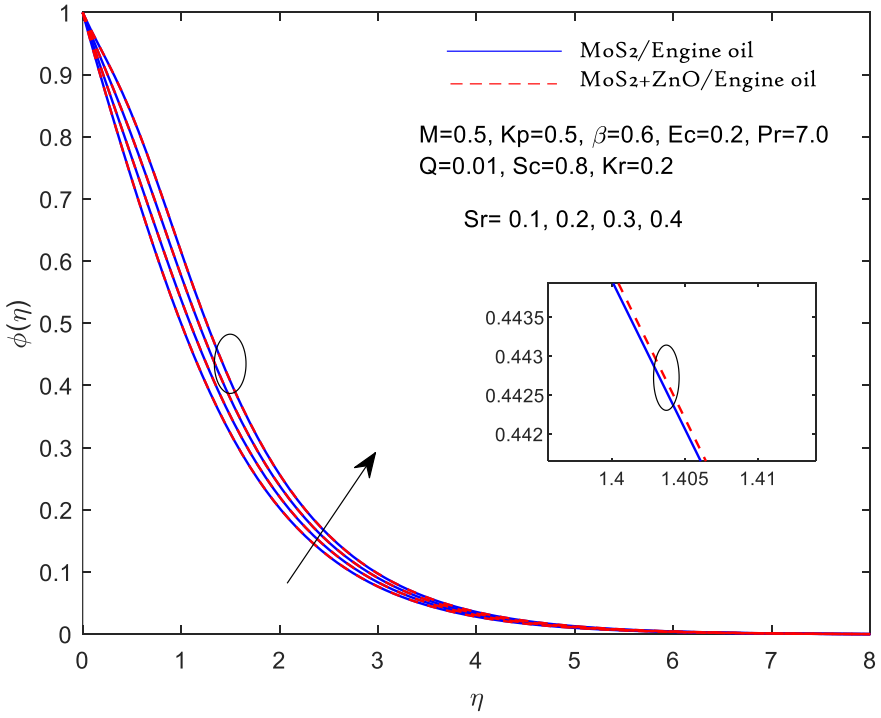

Figure 9. fluctuation with *Sr*.

Preprints.org (www.preprints.org) | NOT PEER-REVIEWED | Posted: 23 April 2024 doi:10.20944/preprints202404.1522.v1

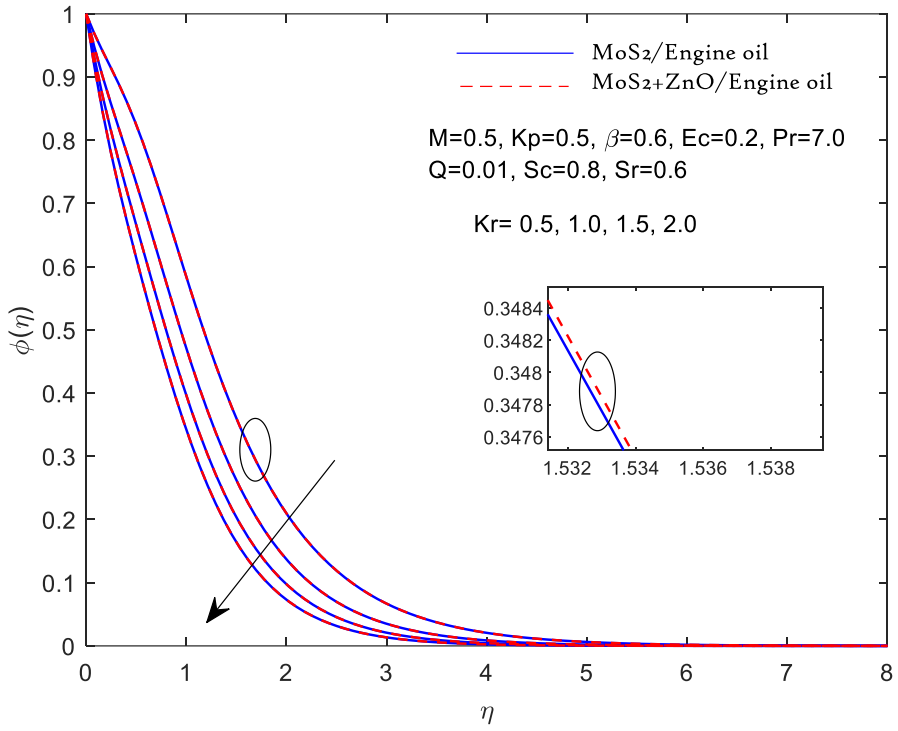

Figure 10. fluctuation with *Kr*.

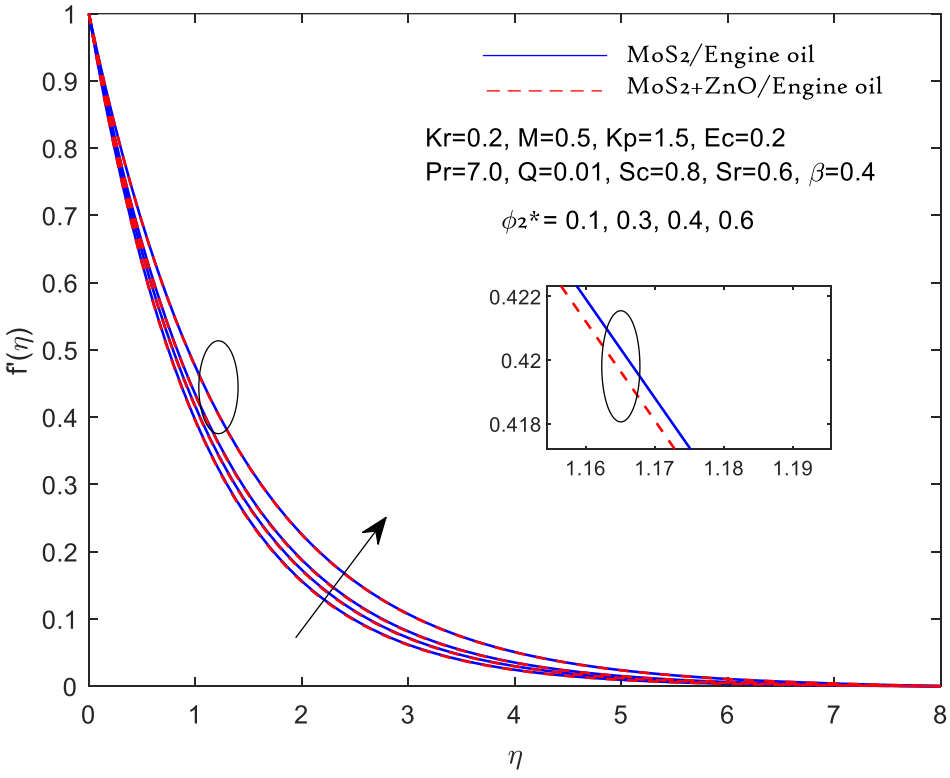

Figure 11. Velocity $f'(\eta)$ fluctuation with $\phi_2{}^*$.

Preprints.org (www.preprints.org) | NOT PEER-REVIEWED | Posted: 23 April 2024 doi:10.20944/preprints202404.1522.v1

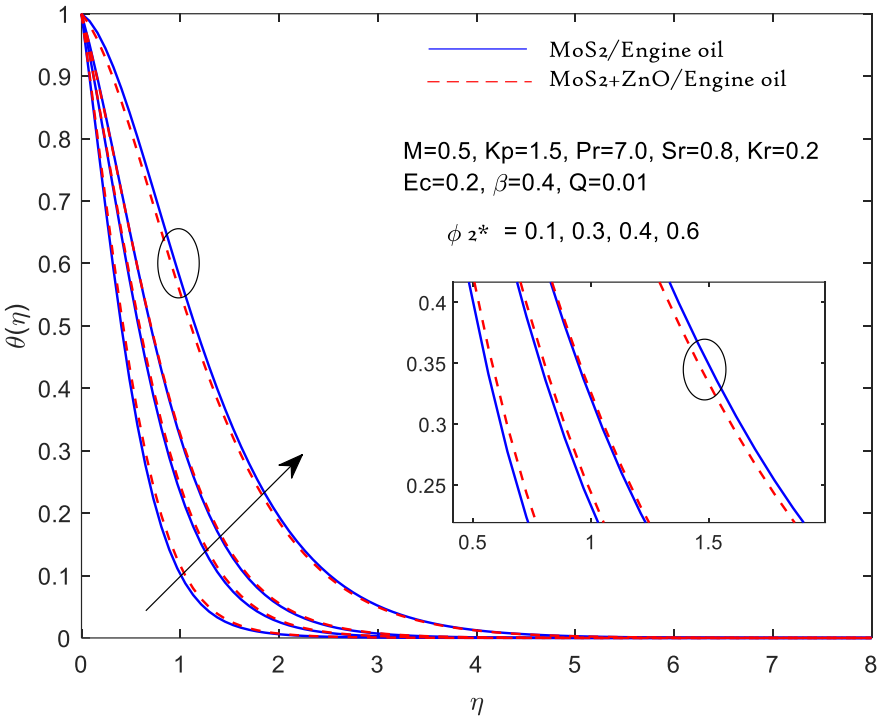

Figure 12. $\theta(\eta)$ fluctuation with ϕ_2 *.

5. Conclusions

The theoretical analysis of Casson hybrid nano lubricant comprising $ZnO + MoS_2$ and engine oil as the base liquid is a model for the heat and mass transportation over a stretching sheet to cross-examine the enhanced thermal efficiency of hybrid nano lubricants. The flow and thermal characteristics are compared with those of simple nano lubricant (MoS_2/Engine oil). In addition, the flow passes through a porous medium in the existence of a magnetic field, thermal dissipation, and heat source. Major findings are described below:

1 The velocity profile diminished against the values of *M*, *Kp*, and β.

2 Temperature profile rises with *Ec* and *Q*, reciprocally goes down to *Pr*.

3 The concentration profile incremented with the value of *Sr* and decremented with the value of *Sc*, and *Kr*.

4 With the increasing value of ϕ_2 * both $f'(\eta)$ and $\theta(\eta)$ increases. But in $\theta(\eta)$ hybrid nano lubricant slows down with the higher value of ϕ_2 *.

Author Contributions: Conceptualization, S.M. and N.B.N.; methodology, S.M.; software, S.M. and N.B.N.; validation, S.M. and N.B.N; formal analysis, S.M. and N.B.N.; writing—original draft preparation, S.M. and N.B.N.; writing—review and editing, N.B.N; supervision. All authors have read and agreed to the published version of the manuscript.

Data Availability Statement: Not applicable.

Conflicts of Interest: The authors declare no conflict of interest.

 doi:10.20944/preprints202404.1522.v1

References

1. Umair, K.; Aurang, Z.; Anuar, I. Impact of Thermal and Activation Energies on Glauert Wall Jet (WJ) Heat and Mass Transfer Flows Induced by ZnO-SAE50 Nano Lubricants with Chemical Reaction: The Case of Brinkman-Extended Darcy Model. Lubricants 2023, 11, 22. [https://doi.org/10.3390/lubricants11010022]
2. Belal, G. N.; Florian, P.; Gerhard, P. Enhancing the Performance of Rapeseed Oil Lubricant for Machinery Component Applications through Hybrid Blends of Nanoadditives. Lubricants 2023, 11, 479. [https://doi.org/10.3390/lubricants11110479]
3. Zia, U.; Ahmad, H.; Musaad, S. A.; Nifeen, H. A.; Sana, S. Significance of Temperature-Dependent Density on Dissipative and Reactive Flows of Nanofluid along Magnetically Driven Sheet and Applications in Machining and Lubrications. Lubricants 2023, 11, 410. [https://doi.org/10.3390/lubricants11090410]
4. Oriana, P. C.; Yamid, N. R.; Vladimir, B. B.; Paulo, C. B.; Tiago, C. Effect of a Metal Conditioner on the Physicochemical Properties and Tribological Performance of the Engine Oil SAE 5W-30. Lubricants 2023, 11, 305. [https://doi.org/10.3390/lubricants11070305]
5. Zawar, H.; Fahad, A.; Ayaz, M.; , Saeed, I.; Significance of Slips and Convective Conditions towards the Non-Newtonian Hybrid Nanofluid Flow over a Bi-Directional Stretching Surface. International Journal of Thermofluids 2023. [https://doi.org/10.1016/j.ijft.2023.100537]
6. Najiyah, S. K.; Norihan M. A.; Ioan, P.; Roslinda, N.; Ezad, H. H.; Nadihah, W.; Three-Dimensional Hybrid Nanofluid Flow and Heat Transfer pasta Permeable Stretching/Shrinking Sheet with Velocity Slip and Convective Condition. Chinese Journal of Physics 2020, 66, 157–171. [https://doi.org/10.1016/j.cjph.2020.03.032]
7. Bilal, S.; Khalil, U. R.; Malik, M. Y.; Arif, H.; Mair, K.; Effects of temperature dependent conductivity and absorptive/generative heat transfer on MHD three dimensional flow of Williamson fluid due to bidirectional non-linear stretching surface. Results in Physics 2017, 7, 204–212.[http://dx.doi.org/10.1016/j.rinp.2016.11.063]
8. Ramzan, M.; Abdullah, D.; Anwar, S.; Poom, K.; Wiboonsak, W.; MHD flow of micropolar and Williamson fluids over a bi-directional stretching sheet. Eur. Phys. J. Plus 2022, 137:869. [https://doi.org/10.1140/epjp/s13360-022-03071-1]
9. Anuar, J.; Roslinda, N.; Ioan, P.; Three-Dimensional Magnetohydrodynamic Mixed Convection Flow of Nanofluids over a Nonlinearly Permeable Stretching/Shrinking Sheet with Velocity and Thermal Slip. Appl. Sci. 2018, 8, 1128. [doi:10.3390/app8071128]
10. Ishtiaq, K.; Amin U. R.; Abdullah, D.; Saeed, I.; Aiman, Z.; Second-order slip flow of a magnetohydrodynamic hybrid nanofluid past a bi-directional stretching surface with thermal convective and zero mass flux conditions. Advances in Mechanical Engineering 2023, 15(2), 1–12. [DOI: 10.1177/16878132221149894]
11. Tanzila, H.; Nadeem, S.; Heat transfer enhancement with Ag–CuO/water hybrid nanofluid. Results in Physics 2017, 7, 2317–2324. [http://dx.doi.org/10.1016/j.rinp.2017.06.034]
12. Awatif, A.; Haneen, H.; Muhammad, B.; Aatif, A.; Numerical study of Williamson hybrid nanofluid flow with thermal characteristics past over an extending surface. Heat Transfer 2022, 1–15. [DOI: 10.1002/htj.22616]
13. Umadevi, S. S.; Anjalidevi, S. P.; Heat Transfer Enhancement Of Cu – Al_2O_3/Water Hybrid Nanofluid Flow Over A Stretching Sheet. Nigerian Mathematical Society 2017, 36(2), 419-433.
14. Ram Prakash, S.; Debasish, G.; Kalidas, D.; Comparative study on hybrid nanofluid flow of Ag– CuO/H_2O over a curved stretching surface with Soret and Dufour effects. Heat Transfer 2022, 1–19. [DOI: 10.1002/htj.22595]
15. Revathi, G.; Sajja, V. S.; Babu, M. J.; Raju, C. S. K.; Shehzad, S. A.; Bapanayya, C.; Entropy optimization in hybrid radiative nanofluid ($CH_3OH + SiO_2 + Al_2O_3$) flow by a curved stretching sheet with cross-diffusion effects. Applied Nanoscience 2021. [DOI: 10.1007/s13204-021-01679-w]
16. Motahar, R.; Anindita, B.; Amalendu, R.; Raghunath, P.; Soret and Dufour effects on entropy generation for AIN and Al_2O_3 Hybrid Nanofluid Flow over past a stretching sheet in porous. Indian Society of Theoretical and Applied Mechanics (ISTAM) 2019, 9-12.
17. Asmat, U. Y.; Nadeem, S.; Wen-Hua, H.; Imran, S.; Sohaib, A.; Sajjad, H.; Thermal charactristics for the flow of Williamson hybrid nanofluid ($MoS_2 + ZnO$) based with engine oil over a streched sheet. Case Studies in Thermal Engineering 2021, 26, 101196. [https://doi.org/10.1016/j.csite.2021.101196]

 doi:10.20944/preprints202404.1522.v1

18. Shami, A. M. A.; Abbas, T.; Al-Zubaidi, A.; Sami, U. K.; Saleem, S.; Analytical assessment of heat transfer due to Williamson hybrid nanofluid (MoS_2 + ZnO) with engine oil base material due to stretched sheet. Case Studies in Thermal Engineering 2023, 15, 103593. [https://doi.org/10.1016/j.csite.2023.103593]
19. Sreedevi, P.; Sudarsana P. R.; Ali Chamkha,; Heat and mass transfer analysis of unsteady hybrid nanofluid flow over a stretching sheet with thermal radiation. SN Applied Sciences 2020,2, 1222. [https://doi.org/10.1007/s42452-020-3011-x]
20. Mubashar, A.; Fahad, M. A.; Ali, H.; Qusain, H.; Abdullah, A.; Sayed, M. E.; Zubair, A.; Laila, A. A.; Ahmed, M. G.; Effect of inclined magnetic field on radiative heat and mass transfer in chemically reactive hybrid nanofluid flow due to dual stretching. Scientific Reports 2023, 13, 7828. [https://doi.org/10.1038/s41598-023-34871-9]
21. Yu-Ming, C.; Muhammad, D. I.; Muhammad, I. A.; Ali, A.; Ferial, G.; Influence of hybrid nanofluids and heat generation on coupled heat and mass transfer flow of a viscous fluid with novel fractional derivative. Journal of Thermal Analysis and Calorimetry 2021, 144, 2057–2077. [https://doi.org/10.1007/s10973-021-10692-8]
22. Asifa, T.; Sadam, K.; Muhammad, B.; Taza, G.; Safyan, M.; Zahir, S.; Ebenezer, B.; Heat and mass transfer together with hybrid nanofluid flow over a rotating disk. AIP Advances 2020, 10, 055317. [doi: 10.1063/5.0010181]
23. Shanmugapriya, M.; Sundareswaran, R.; Senthil Kumar, P.; Heat and Mass Transfer Enhancement of MHD Hybrid Nanofluid Flow in the Presence of Activation Energy. International Journal of Chemical Engineering 2021. https://doi.org/10.1155/2021/9473226]
24. Sohail, A.; Kashif, A.; Muhammad, R.; Muhammad, A.; Heat and mass transfer attributes of copper–aluminum oxide hybrid nanoparticles flow through a porous medium. Case Studies in Thermal Engineering 2021, 25, 100932. [https://doi.org/10.1016/j.csite.2021.100932]
25. Abdulmajeed, A.; Numerical study on heat and mass transport enhancement in MHD Williamson fluid via hybrid nanoparticles. Alexandria Engineering Journal 2022, 16, 8343–8354. [https://doi.org/10.1016/j.aej.2022.01.041]
26. Gohar.; Tahir, S. K.; Ndolane, S.; Abir, M.; Ameni, B.; Heat and Mass Transfer of the Darcy-Forchheimer Casson Hybrid Nanofluid Flow due to an Extending Curved Surface. Journal of Nanomaterials 2022. [https://doi.org/10.1155/2022/3979168]
27. Alia, F.; Zaiba, A.; Faizana, M.; Zafara, S.S.; Shalan, A.; Nehad, A. S.; Jae, D. C.; Heat and mass exchanger analysis for Ree-Eyring hybrid nanofluid through a stretching sheet utilizing the homotopy perturbation method. Case Studies in Thermal Engineering 2024, 54, 104014. [https://doi.org/10.1016/j.csite.2024.104014]
28. Wei-Feng, X.; Shafiq, A.; Naveed, K. Md.; Hijaz, A.; Aysha, R.; Jamel, B.; Tuan, N. G.; Heat and mass transfer analysis of nonlinear mixed convective hybrid nanofluid flow with multiple slip boundary conditions. Case Studies in Thermal Engineering 2022, 32, 101893. [https://doi.org/10.1016/j.csite.2022.101893]
29. Saeed, D.; Mohammadreza, N. R.; Ioan, P.; A novel hybridity model for TiO_2- CuO/water hybrid nanofluid flow over a static/moving wedge or corner. Scientific Reports 2019, 9, 16290. [https://doi.org/10.1038/s41598-019-52720-6]
30. Saqib, Md.; Ilyas, K.; Sharidan, S.; Application of fractional differential equations to heat transfer in hybrid nanofluid: modeling and solution via integral transforms. Advances in Difference Equations 2019, 52. [https://doi.org/10.1186/s13662-019-1988-5]